Scientific Research Publishing

Advances in Materials Physics and Chemistry, 2022, 12, 58-67
https://www.scirp.org/journal/ampc
ISSN Online: 2162-5328
ISSN Print: 2162-531X

Development of a Graphite Coating and Its Transfer from Batch to Coil Process for Application in PEMFC for Hydrogen-Powered Vehicles

Maurizio Giorgio[1*], Maximilian Steinhorst[1,2], Slavcho Topalski[1], Teja Roch[1], Christoph Leyens[1,2]

[1]Fraunhofer Institute for Material and Beam Technology IWS, Dresden, Germany
[2]Institute of Materials Science, Technische Universität Dresden, Dresden, Germany
Email: *maurizio.giorgio@iws.fraunhofer.de

How to cite this paper: Giorgio, M., Steinhorst, M., Topalski, S., Roch, T. and Leyens, C. (2022) Development of a Graphite Coating and Its Transfer from Batch to Coil Process for Application in PEMFC for Hydrogen-Powered Vehicles. *Advances in Materials Physics and Chemistry*, **12**, 58-67.
https://doi.org/10.4236/ampc.2022.124005

Received: December 30, 2021
Accepted: April 21, 2022
Published: April 24, 2022

Abstract

In the present paper, coating systems consisting of a metallic corrosion barrier and a conductive graphitic carbon layer were deposited by a DC vacuum arc process. The coatings were developed in a batch process for application in the polymer electrolyte membrane fuel cell (PEMFC), and transferred to a continuous coil process to facilitate industrial mass production. The coating samples in the coil process had to achieve comparable results to the samples produced in the batch process, to meet the requirements of the environment prevailing in the fuel cell. The transfer to roll-to-roll processes is a crucial factor for commercial upscaling of PEMFC production. The experimental results showed that the electrical conductivity and corrosion resistance of the samples in the coil process were significantly improved compared to the uncoated base material and showed comparable performance to batch coated samples. X-ray photoelectron spectroscopy (XPS) was performed to determine the depth profile and the surface composition. Additional measurements were recorded for the contact resistances using the four-wire sensing method as well as corrosion resistance using potentiodynamic methods.

Keywords

Graphit-Like-Carbon (GLC), Batch Coating, Coil Coating, Bipolar Plate

1. Introduction

Because of the current discussion on reducing greenhouse gas emissions worldwide, a new Federal Climate Protection Act was passed in the Federal Republic

of Germany in mid-2021. It stipulates that Germany must reduce greenhouse gas emissions by 65 percent until 2030 compared to emissions in the year 1990. Additionally, there are plans to become greenhouse gas neutral by 2045. To achieve these ambitious goals, a large number of developments and technologies must be made available in a wide range of areas [1]. One possibility in the mobility sector, in addition to all-electric power trains, is the development of fuel cell powered vehicles based on PEMFCs. The PEMFC is already established in the fuel cell market and, according to economic analyses, will increase its market potential even further [2].

The specific advantages, such as the use of a solid electrolyte, high current density, and good dynamic behavior, make them a promising solution in hydrogen-powered vehicles [3]. Weight and space are critical in passenger cars, so metallic bipolar plates (BPPs) can have specific advantages over other materials. The fuel cell serves as a converter from chemical to electrical energy and consists of a cell stack, the individual cells of which are composed of a membrane electrode assembly (MEA) consisting of two gas diffusion layers and a catalyst-coated membrane as well as an anodic and cathodic bipolar plate [4] as shown in **Figure 1**.

In contrast to electrolysis, where water is converted into hydrogen and oxygen, in a PEMFC a reverse reaction takes place by feeding the process media hydrogen and oxygen [5] [6]. In this process, besides electricity, which is the primary goal to be achieved with the fuel cell, water vapor and heat are also yielded as by-products [5] [7]. In a PEMFC, the solid electrolyte (*i.e.* the membrane) spatially separates the reaction steps of the anodic partial reaction (oxidation/electrode discharge, Equation (1)) from the cathodic partial reaction (reduction/electrode uptake, Equation (2)) [5].

$$2H_2 + 4H_2O \rightarrow 4H_3O^+ + 4e^- \quad (1)$$

$$O_2 + 4H_3O^+ + 4e^- \rightarrow 6H_2O \quad (2)$$

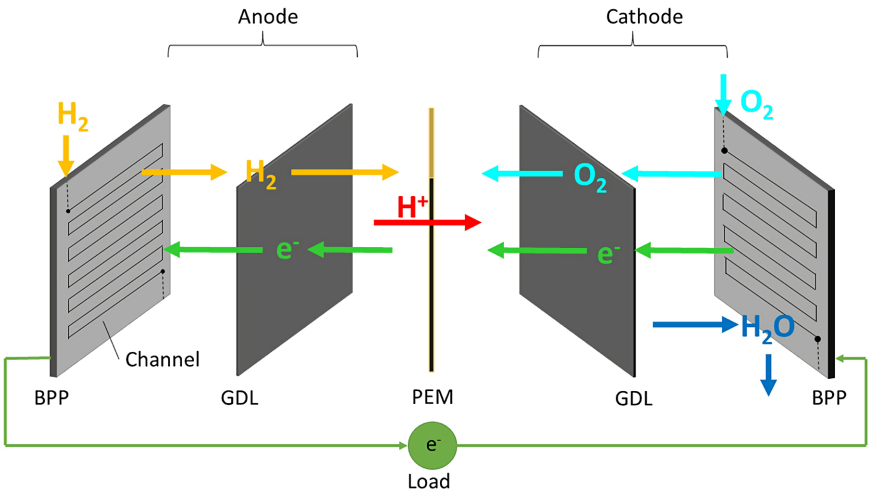

Figure 1. Schematic partial section of a PEMFC.

From this follows the total reaction in a PEMFC (redox reaction/cell reaction, Equation (3)).

$$2H_2 + O_2 \rightarrow 2H_2O \tag{3}$$

The oxidation of hydrogen on the anode side creates an excess of H^+ ions in the fuel cell, which results in an acidic environment [5] [8]. Due to relatively low material costs and good formability, thin foils made of stainless steel are suitable for the bipolar plates [9]. However, the stainless steel requires surface modification due to its passivation layer, which reduces its electrical conductivity. Due to the aggressive environment in the fuel cell, a corrosion-resistant layer is also required [10]. The Surface coating is necessary, on the one hand, to increase the service life, which is affected by corrosion processes. On the other hand, the coating can increase the power density that is lowered by the electrical contact resistances. In addition, coating defects caused by forming after coating must not affect the fuel cell system, otherwise the fuel cell would be poisoned by leaching out alloy components. The formability of the coating places high demands on the coating system [11] [12] [13] [14].

A variety of technologies is available for coating materials. The process used here is physical vapor deposition (PVD) [15]. This process can be implemented using the four different techniques of evaporation, sputtering, arc evaporation, and ion plating [16]. For the coatings in the processes carried out here, cathodic arc evaporation was used. This process had to be designed in such a way that the coating of the bipolar plate could be evolved from a single-component coating to a coil coating process, allowing mass production of the bipolar plate in a cost-effective manner [17]. In a roll-to-roll coating process, in which the coil is subsequently formed, joined and separated (so-called pre-coating), the coating must, after these production steps, still achieve a performance comparable to coatings applied to prefabricated bipolar plates (post-coating).

There are many studies dealing with the topic of coatings on BPP for PEMFC and their characterization. Extensive research examines the fields of fuel cell functions, cell reactions as well as simulation methods of media flows, consideration of interfacial reactions, design of flowfield geometries or influences of cyclic operations in in-situ experiments [18] [19] [20] [21]. In this paper, we study the production aspects of a carbon based coating for metallic bipolar plates. The knowledge gained in this work contributes to transferring a carbon-based coating to a roll-to-roll process, thus contributing to upscaling of BPP production for commercial use of fuel cell vehicles.

2. Experiments

2.1. Coating Processes

The layer systems used here are based on carbon thin film and are generally amorphous or nano crystalline, unless they are deposited as diamond. The bonding properties in the layer systems are composed of graphitic (sp^2) and diamond-like (sp^3) bonding components. In the case of the predominantly di-

amond-like bonds, these coatings are referred to as diamond-like-carbon (DLC), which are very hard and are mainly used as wear protection for components. Because of their poor conductivity, the focus in fuel cell coatings is on producing a high graphitic content and thus graphite-like-carbon (GLC). The coating system, consisting of a corrosion-resistant chromium layer and a conductive carbon layer, is applied to the base material, AISI 316L stainless steel, as shown in Figure 2.

The coating was carried out in an industrial size PVD coater from the company Metaplas, type MZR 373. The standard GLC coating procedure is as follows: first, the chamber and the samples are heated to approx. 300˚C, and this temperature is maintained during the subsequent process steps. Next, plasma cleaning is performed, followed by the deposition of an intermediate metallic layer and the deposition of a carbon layer. The coating is carried out at a pressure of 1×10^{-3} mbar.

2.2. Batch Processes

In the batch process, samples of plain sheets and prefabricated bipolar plates were coated. After installation of the samples in holders manufactured for this purpose, the coating chamber was loaded and the samples were coated according to the following process sequence:

After an initial bake-out of the coating chamber and the samples, a plasma cleaning was performed to remove the passivation layer of the stainless steel. Then the chromium intermediate layer was applied, followed by the carbon coating. The coating times of the individual process steps were very short, about 2 minutes each. Since the samples were coated in a plant-specific, twofold rotational movement, considerable differences in coating thickness occur here due to the coating dynamics, which were in the range of approx. 80 - 120 nm.

2.3. Coil Processes

For the coil processes, the batch coating chamber was converted by installing an external coil module. A coil coating line is simulated with the take-up and take-off roll installed in the coil module, and a drum roll installed inside the coating chamber. Analogous to the sequence of steps in the batch process, the process steps in coil coating are carried out one after the other.

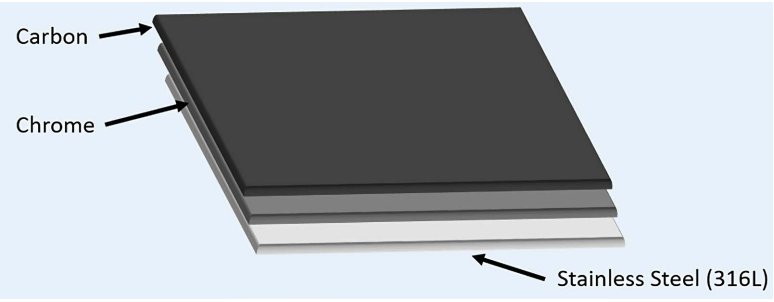

Figure 2. Schematic diagram of the graphite-like-carbon layer system.

This means that after the first bake-out step of the line, the steel coil must be rewound after each coating step. For example, in the first process step of plasma cleaning, a certain length of the material is unwound and then rewound again to subsequently carry out the chromium coating and then the carbon coating. For the coil and batch coatings, material thicknesses of 0.1 mm were investigated and the coil speeds during the coating was approx. 2.3 m/min.

3. Characterization

X-ray photoelectron spectroscopy (XPS, PHI Quantum 2000) of the overview spectrum was acquired by a focused monochromatic X-ray source (Al-Kα, 1486.68 eV) with a beam diameter of 100 µm and a power of 100 W from an area of about 1.4 × 0.4 mm^2. The depth profile was measured using an Ar ion beam with an energy of 1 kV scanning over the area of 3 × 3 mm^2.

The ablation rate is 1.4 nm/min for SiO_2. In this case, the spectra were recorded with a beam diameter of 200 µm and a power of 50 W. Contact resistance measurements were taken by four-wire measurement between two gold-coated copper dies with an area of 2 × 2 mm^2 and a pressure of about 50 N/cm^2. Corrosion measurements were done with a potentiostat (Methrom Autolab) using the three-electrode electrochemical measurement method with a 0.05 mol/l H_2SO_4 electrolyte at room temperature with a polarization speed of 0.5 mV/s and a measurement area of approximately 1.48 cm^2.

4. Results and Discussion

If the coating is applied before the forming process, the adhesive strength of the coating must be high enough to avoid delamination of the coating. Commercially manufactured bipolar plates have a high degree of forming due to their fine channel geometries, which thins out the base material at the channel flanks. This leads to high stresses in the base material and in the coating. The forming processes can cause shear cracks in the coating in the area of the channel flanks. However, passivation of the stainless steel base material also occurs at the defective areas. This effect is not occurring in other base materials, which are not suitably corrosion-resistant for the requirements of this type of fuel cell. For this reason, this process cannot be transferred to materials that are not resistant to corrosion without further research.

The overview spectrum in **Figure 3** shows the qualitative and quantitative detection of the chemical elements in the surface region of the GLC sample. It can be seen that the largest portion of 93.1 at.% is carbon, as also shown in **Table 1**. Another 5.2 at.% is oxygen and the other contaminations are negligible. This result indicates that the surface mainly consists of carbon and oxygen, and the base material (SS316L with contents of iron, chromium and nickel) is not detectable.

In the depth profile of the XPS measurement (**Figure 4**, left), a clearly pronounced layer system can be seen. A separate carbon layer is clearly visible down

Table 1. Atomic concentration table of the XPS measurement.

Electron shell	Atomic Concentration GLC Surface
	Amount [at.%]
C1s	93.1
N1s	0.5
O1s	5.2
Si2p	0.2
Ca2p	0.1
Cr2p	0.8
Zn2p3	0.1

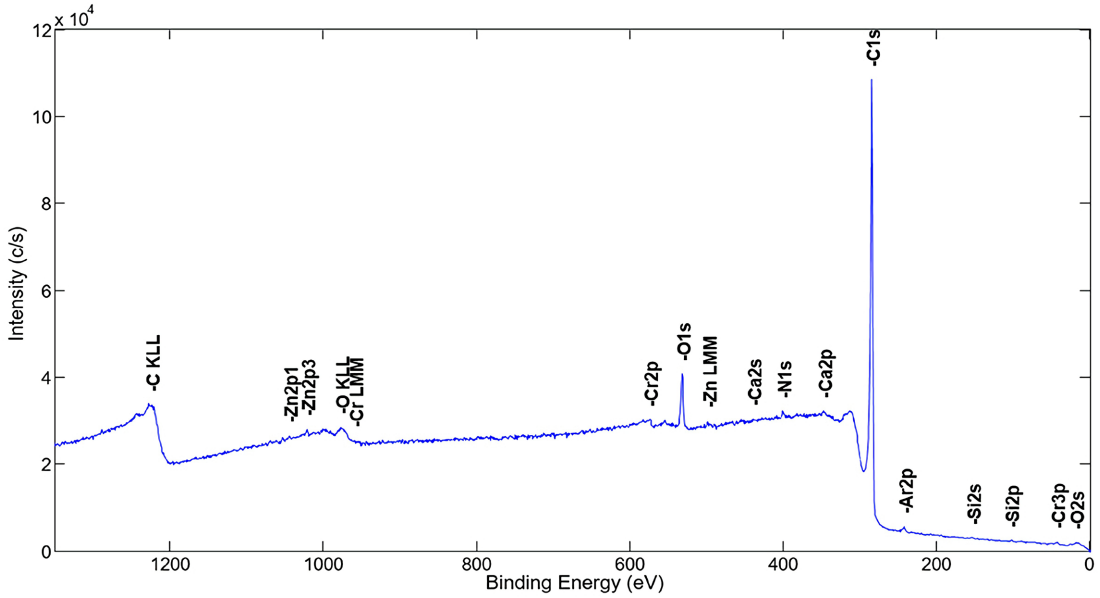

Figure 3. Overview spectrum of the surface region of the GLC layer system from coil coating process.

to a depth of approx. 60 nm. After a small transition area of carbon and chromium, the chromium layer continues to a depth of approx. 130 nm. Plasma pre-cleaning removes the material but as can be seen from the oxygen peak, the oxygen layer is not completely eliminated. As can be seen from the transition from carbon to chromium, the carbon layer is firmly anchored, which can also be seen in the forming results (not published here). Iron is not present on the surface, which can be seen in the overview spectra as well as in the depth profile. **Figure 4**, right, shows the XPS measurement of a batch coating, which is comparable to the measurement of the coil coating. The coating of the coil process is even thicker than that of the batch process, and thus allows even faster coil speeds. Comparable coating in the transfer from batch to coil processes was achieved.

The carbon-based coatings significantly reduce the contact resistance of stainless steel, and the coating tests in the batch and coil processes show comparable

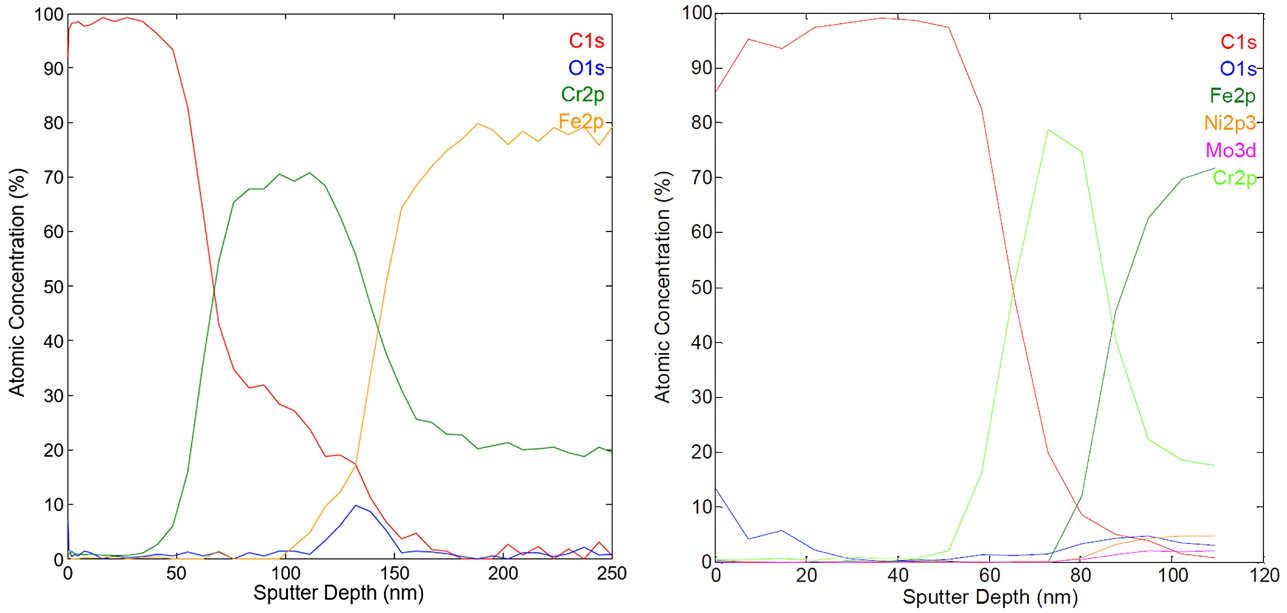

Figure 4. XPS depth profile of the GLC layer system with the relevant elements from coil coating process (left) and batch coating process (right).

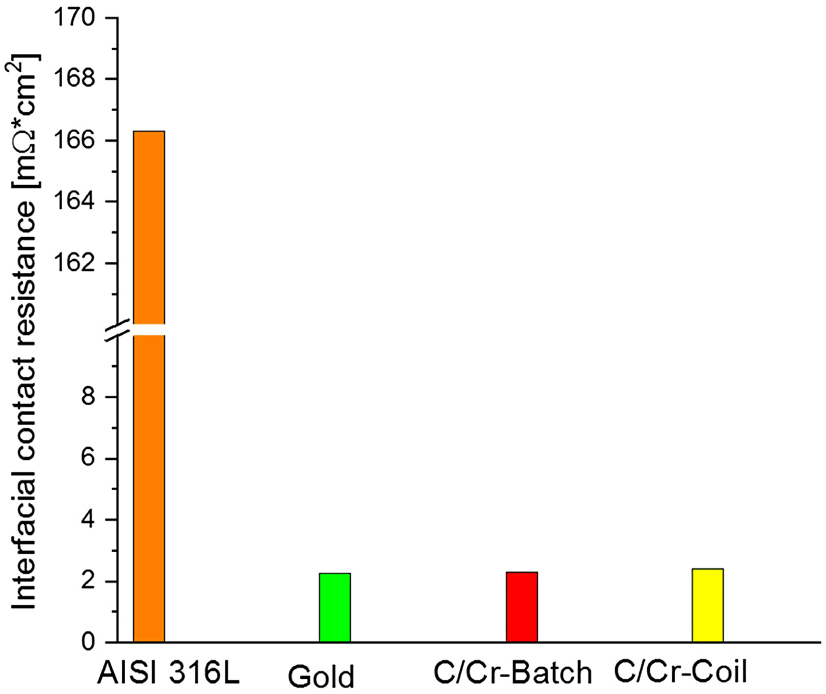

Figure 5. Contact resistance measurements of the carbon/chrome layer in batch and coil process, gold layer, and the SS316L.

contact resistances, which are in the range of gold-coated stainless-steel sheets, as shown in Figure 5 (C/Cr-Batch and C/Cr-Coil). The corrosion current density of the 0.1 mm thick samples was significantly reduced by the coating. Carbon coating with an intermediate chromium layer shows an increase in corrosion current at about 1.2 V voltage shown in Figure 6 (C/Cr-Batch and C/Cr-Coil).

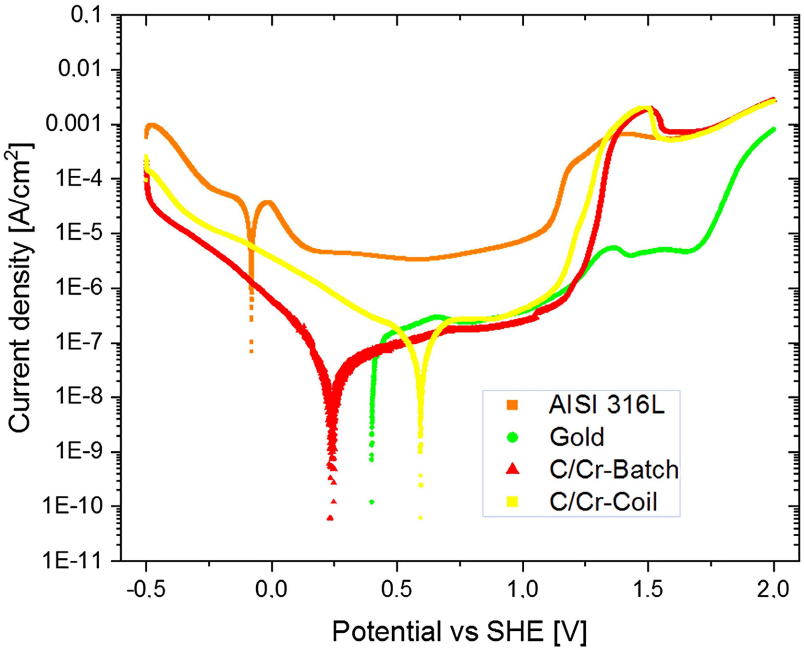

Figure 6. Current density potential curves of the carbon/chrome layer in batch and coil process, gold layer, and the SS316L

Coating systems with alternative metallic interlayers can potentially further improve the corrosion properties of the coatings. However, the performances of a carbon-based coating produced in a batch or coil coating process are comparable and can reach electrical contact resistances and corrosion current densities (approx. between 0.25 and 1.0 V) comparable to gold.

5. Conclusion

The upscaling of a carbon coating processes with a chromium interlayer from batch to coil has been successfully demonstrated. Contact resistance and corrosion measurements demonstrated the good performance of the coatings. Carbon-based coatings deposited in PVD coil processes show high potential for industrial mass production of steel coil to produce bipolar plates with pre-coating. An important aspect is that the cost of producing bipolar plates can be greatly reduced by using coil processes rather than batch process. Further investigations to transfer the coatings to a steel coil line are planned. Additionally, further research in the field of alternative interlayers has the potential to increase the corrosion resistance of metallic BPP.

Acknowledgements

Maurizio Giorgio would like to thank the Fraunhofer Institute for Material and Beam Technology in Dortmund for their support, as well as the Institute for Material Science at the Technical University of Dresden. He would also like to thank all project partners from miniBIP II (Reference no. 03ETB007B) and the Fraunhofer internal research project HOKOME.

Conflicts of Interest

The authors declare no conflicts of interest regarding the publication of this paper.

References

[1] Appunn, K., Eriksen, F. and Wettengel, J. (2021) Germany's Greenhouse Gas Emissions and Energy Transition Targets. Clean Energy Wire. https://www.cleanenergywire.org/

[2] Businesswire (2021) The Global Fuel Cell Market: Size, Share & Trends Analysis by Product, Application and Region (2018-2025)—Projected to Grow at a CAGR of 20.9%—ResearchAndMarkets.com. https://www.businesswire.com/news/home/20181204005535/en/%20Glob-al-Fuel-Cell-Market-Size-Share-Trends%20/

[3] Porstmann, S., Scheffler, S. and Maika, C. (2018) Manufacturing Technologies for PEMFC Stack Components and Stacks. Report—Business Studies—Fit-4-AMandA D1.2 (GA#735606).

[4] Porstmann, S., Wannemacher, T. and Richter, T. (2019) Overcoming the Challenges for a Mass Manufacturing Machine for the Assembly of PEMFC Stacks. *Machines*, **7**, Article No. 66. https://doi.org/10.3390/machines7040066

[5] Kurzweil, P. (2020) Angewandte Elektrochemie: Grundlagen, Messtechnik, Elektroanalytik, Energiewandlung, technische Verfahren. Springer-Verlag, Wiesbaden. https://doi.org/10.1007/978-3-658-32421-6

[6] Klell, M., Eichlseder, H. and Trattne, A. (2018) Wasserstoff in der Fahrzeugtechnik. Springer-Verlag, Wiesbaden. https://doi.org/10.1007/978-3-658-20447-1

[7] Behr, A., Agar, D.W., Jörissen, J. and Vorholt, A.J. (2016) Einführung in die Technische Chemie. Springer-Verlag, Berlin. https://doi.org/10.1007/978-3-662-52856-3

[8] Jin, J., Zhu, Z. and Zheng, D. (2017) Influence of Ti Content on the Corrosion Properties and Contact Resistance of CrTiN Coating in Simulated Proton Exchange Membrane Fuel Cells. *International Journal of Hydrogen Energy*, **42**, 11758-11770. https://doi.org/10.1016/j.ijhydene.2017.02.014

[9] Leng, Y., Ming, P., Yang, D. and Zhang, C. (2020) Stainless Steel Bipolar Plates for Proton Exchange Membrane Fuel Cells: Materials, Flow Channel Design and Forming Processes. *Journal of Power Sources*, **451**, Article ID: 227783. https://doi.org/10.1016/j.jpowsour.2020.227783

[10] Karimi, S., Fraser, N., Roberts, B. and Foulkes, F.R. (2012) A Review of Metallic Bipolar Plates for Proton Exchange Membrane Fuel Cells: Materials and Fabrication Methods. *Advances in Materials Science and Engineering*, **2012**, Article ID: 828070. https://doi.org/10.1155/2012/828070

[11] Netwall, C.J., Gould, B.D., Rodgers, J.A., Nasello, N.J. and Swider-Lyons, K.E. (2013) Decreasing Contact Resistance in Proton-Exchange Membrane Fuel Cells with Metal Bipolar Plates. *Journal of Power Sources*, **227**, 137-144. https://doi.org/10.1016/j.jpowsour.2012.11.012

[12] Lu, J.L., Abbas, N., Tang, J., Hu, R. and Zhu, G.M. (2019) Characterization of Ti_3SiC_2-Coating on Stainless Steel Bipolar Plates in Simulated Proton Exchange Membrane Fuel Cell Environments. *Electrochemistry Communications*, **105**, Article ID: 106490. https://doi.org/10.1016/j.elecom.2019.106490

[13] Cho, E.A., Jeon, U.S., Hong, S.A., Oh, I.H. and Kang, S.G. (2005) Performance of a 1kW-Class PEMFC Stack Using TiN-Coated 316 Stainless Steel Bipolar Plates.

Journal of Power Sources, **142**, 177-183.
https://doi.org/10.1016/j.jpowsour.2004.10.032

[14] Wang, X.X., Swihart, M.T. and Wu, G. (2019) Achievements, Challenges and Perspectives on Cathode Catalysts in Proton Exchange Membrane Fuel Cells for Transportation. *Nature Catalysis*, **2**, 578-589. https://doi.org/10.1038/s41929-019-0304-9

[15] Baptista, A., Silva, F.J.G., Porteiro, J., Míguez, J.L., Pinto, G. and Fernandes, L. (2018) On the Physical Vapour Deposition (PVD): Evolution of Magnetron Sputtering Processes for Industrial Applications. *Procedia Manufacturing*, **17**, 746-757. https://doi.org/10.1016/j.promfg.2018.10.125

[16] Mattox, D.M. (2010) Handbook of Physical Vapor Deposition (PVD) Processing. 2nd Edition, William Andrew, Oxford.

[17] Alo, O.A., Otunniyi, I.O. and Pienaar, H. (2019) Manufacturing Methods for Metallic Bipolar Plates for Polymer Electrolyte Membrane Fuel Cell. *Materials and Manufacturing Processes*, **34**, 927-955. https://doi.org/10.1080/10426914.2019.1605170

[18] Wang, K., Liu, Z.C. and Yang, J.G. (2021) Numerical Study of Gas-Liquid Two-Phase Flow in PEMFC Cathode Flow Channel with Different Diffusion Layer Surface Structure. *Journal of Power and Energy Engineering*, **9**, 106-117. https://doi.org/10.4236/jpee.2021.911006

[19] Wen, C., An, J., Hau, J., Lv, X., Ding, L. and Qiu, X. (2021) Corrosion Behavior of Au Coating on 316L Bipolar Plate in Accelerated PEMFC Environment. *International Journal of Electrochemical Science*, **16**, Article No. 211147. https://doi.org/10.20964/2021.11.50

[20] Yang, L.X., Liu, R.J., Wang, Y., Liu, H.J., Zeng, C.L. and Fu, C. (2021) Corrosion and Interfacial Contact Resistance of Nanocrystalline β-Nb_2N Coating on 430 FSS Bipolar Plates in the Simulated PEMFC Anode Environment. *International Journal of Hydrogen Energy*, **46**, 32206-32214. https://doi.org/10.1016/j.ijhydene.2021.06.207

[21] Müller, M.V., Giorgio, M., Hausmann, P., Kinlechner, L., Heinzel, A. and Schwämmlein, J. (2021) Investigation of the Effect of Carbon Post- vs Pre-Coated Metallic Bipolar Plates for PEMFCs—Start-Up and Shut-Down. *International Journal of Hydrogen Energy*, **47**, 8532-8548. https://doi.org/10.1016/j.ijhydene.2021.12.179